



## Semarak International Journal of Chemical Process Engineering

Journal homepage:  
<https://semarakilmu.my/index.php/sijcpe/index>  
ISSN: 3036-020X



# Integration of Air Splitters and Air Deflectors in Vertical Roller Mills: A Computational Fluid Dynamic–Discrete Particle Method Approach to Improve Milling Performance

Arwan Suryadi Pramanta<sup>1,\*</sup>, Grandis Belva Ardana<sup>1</sup>, Ahmad Dzaky Harahap<sup>1</sup>, Rona Najma Athif<sup>1</sup>, Rahmat Agustian Pamungkas<sup>2</sup>, Haniif Prasetiawan<sup>1</sup>

<sup>1</sup> Department of Chemical Engineering, Faculty of Engineering, State University of Semarang, Semarang, Central Java, Indonesia

<sup>2</sup> Department of Mechanical Engineering, Faculty of Engineering, Semarang State University, Semarang, Central Java, Indonesia

### ARTICLE INFO

#### Article history:

Received 26 June 2025

Received in revised form 22 July 2025

Accepted 30 July 2025

Available online 4 August 2025

#### Keywords:

*Discrete Phase Model; particle tracking efficiency; multiphase flow*

### ABSTRACT

This study examines the efficiency of particle tracking using the Discrete Phase Model (DPM) in multiphase flow simulations by comparing three configuration scenarios: serial mode (without parallel), parallel mode with default loop-factor settings, and parallel mode with reduced loop-factor. A total of 22,118 particles were tracked in each scenario to evaluate the number of particles that completed their trajectories (escape), those that did not complete (incomplete), and those trapped in parallel loops (incomplete parallel). Efficiency was calculated using the ratio of escape particles to the total number of particles tracked. The results showed that the parallel scenario with the default loop factor had the highest efficiency rate, approximately 62%, where most particles successfully left the simulation domain. In contrast, the serial mode only showed an efficiency of around 35%, indicating that many particles failed to complete their trajectories due to iteration limitations. Meanwhile, reducing the loop factor in parallel mode did decrease the number of incomplete particles. Still, it increased the number of particles trapped in the parallel process, reducing efficiency to around 51%. These findings indicate that using the parallel mode with standard settings provides an optimal balance between computational speed and particle tracking reliability. This configuration is recommended to enhance accuracy and efficiency in large-scale multiphase flow simulations, especially when the number of tracked particles is sufficiently large. Thus, selecting the appropriate parallel strategy significantly impacts the performance and quality of DPM-based simulation results.

## 1. Introduction

Vertical Roller Mill (VRM) is a large grinding equipment integrating various functions such as material crushing, transportation, drying, and separating [1]. VRM has many advantages, including high grinding efficiency, low energy consumption, minimal dust emission, and easy adjustment of

\* Corresponding author.

E-mail address: [arwan978@students.unnes.ac.id](mailto:arwan978@students.unnes.ac.id)

product fineness [2]. With the continuous development of technology, VRM has been widely applied in processing various applications in industries such as mining, building materials, metallurgy, and chemical engineering due to its superior powder grinding ability, making significant contributions to the national economy [3]. VRM consists of several key components, including a classification drive device, a grinding roller device, a grinding table device, and a pressure lubrication device [4]. In the design of VRM, the air splitter functions to distribute gas across the surface of the table and rollers, while the air deflector directs the flow back to the separating zone; these two components determine the turbulence characteristics and particle velocity in the grinding disc [5]. Recent CFD studies have shown that modifying the geometry of the splitter and deflector, such as their number and angle, can minimize air ingress and optimize pressure distribution, thereby increasing throughput and reducing specific energy consumption [6].

As mentioned earlier, many researchers have conducted relevant studies to address the problems. Xu *et al.*, conducted a numerical simulation analysis in which they blocked some low-flow nozzle rings to increase the wind speed in the nozzle ring, which led to better flow distribution and pressure drop in the mill [7]. By changing the air inlet arrangement, they successfully stabilized the flow field. Hu *et al.*, found that the air ring structure is a key factor affecting the total pressure resistance of the TRM53.4 mill [8]. Installation blades inside the air ring, increase the ventilation area, thereby reducing the wind speed to an appropriate level and reducing the overall pressure performance of the mill. In their study, Liu *et al.*, conducted a numerical simulation study on VRM. The study found that increasing the system air volume, rotation speed, number of blades, and top shell angle can increase the pressure loss in the VRM, which leads to higher energy consumption [9]. Therefore, it is essential to optimize both the operational parameters and the structure of the VRM to reduce energy consumption. In their study, Altun *et al.*, found that the rotor speed of the classifier is inversely related to the product yield and product size [10]. By integrating the relationship between the obtained single grinding parameters and the mineral characterization results, they established the first basis for assessing the performance of the VRM model in Fatahi *et al.* DPM and GBM algorithms showed that working pressure, mill fan speed, and feed rate were the main factors affecting the differential pressure (DP) in VRM. GBM successfully predicted DP with high accuracy ( $R^2 = 0.9684$ ). SHAP analysis revealed a non-linear relationship between the variables, while DPM confirmed that the blade design affected the classification efficiency and flow stability [11]. The results showed that as the rotational speed of the grinding table increased, particles were more likely to spill off the table, resulting in less particle accumulation and a thinner particle layer, but this also increased the wear on the outer ring. In addition, using a higher retaining ring reduced the performance of the VRM, causing more severe grinding fluctuations and greater wear. Liu *et al.*, conducted a crushing study on VRM using DEM and a bound particle model. The results showed that increasing the rotational speed of the grinding table reduced the particle crushing rate [12]. In addition, increasing the feed rate and the distance between the grinding roller and the grinding table causes the particle breakage rate to increase initially, followed by a subsequent decrease, thereby increasing particle movement and VRM output. Therefore, this study integrates CFD–DPM coupling with a variable triple-ring splitter design and an optimal deflector angle of  $5^\circ$  to quantitatively maximize the specific energy efficiency and suppress the product size variance in the Vertical Roller Mill.

## 2. Methodology

### 2.1 Geometry

Geometry represents a standard industrial configuration, including the nozzle ring system, the main pathway for gas flow into the milling chamber. The size and placement of each component are

designed to support an efficient milling process. The geometry of the Vertical Roller Mill (VRM) is illustrated in Figure 1.

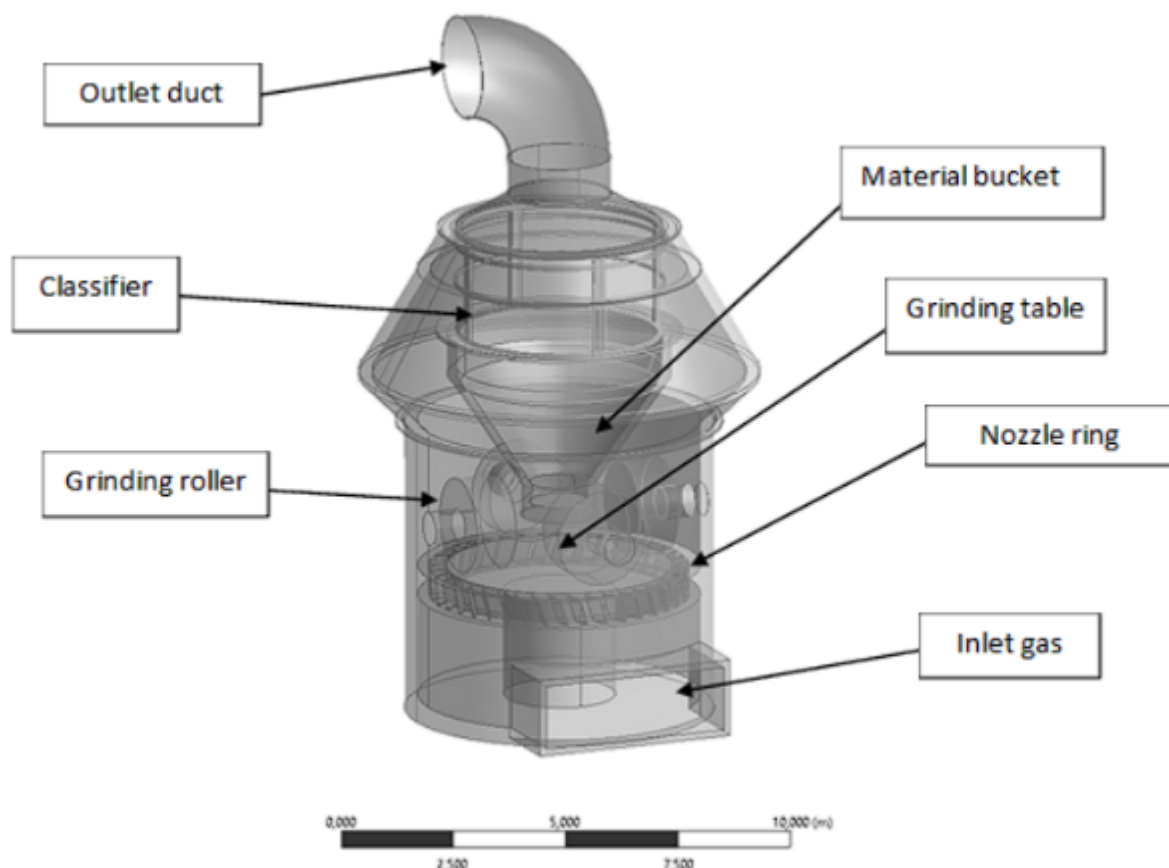


**Fig. 1.** Vertical roller mill (VRM)

The geometry of the vertical roller mill (VRM) used features a grinding table diameter of 5 meters and an overall system height of 12.28 meters. The main dimensions of the VRM are presented in Table 1. The initial configuration reflects a standard grinding design, including a nozzle ring system that is the primary pathway for gas flow into the grinding chamber. The geometry of the main parameters of the VRM is illustrated in Figure 2.

**Table 1**

Main dimensions of the VRMs

Dimension	Length, mm
Height/A	12283
Diameter/B	6310
Inlet port length/C	4300
Inlet port height/D	1430
Grinding table diameter/E	5000
Outlet diameter/F	2291

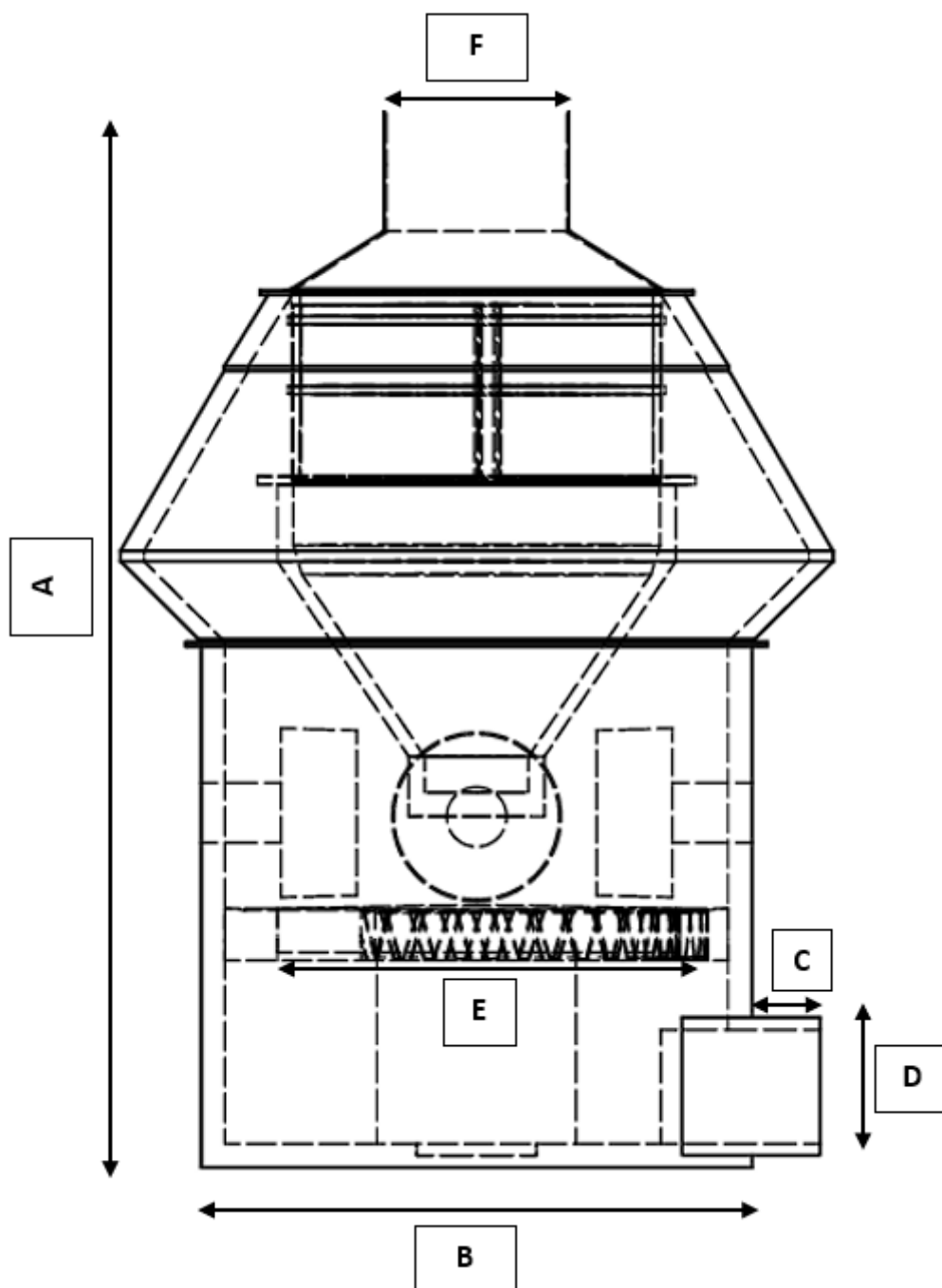


**Fig. 2.** Geometric parameters of Vertical Roller Milling Machine (VRM)

Modifications were made to the gas flow system by adding an air splitter and air deflector components to evaluate the impact of geometric configuration changes on the vertical roller mill (VRM) performance. The addition of the air splitter and air deflector aims to change the direction and distribution of the gas before it enters the grinding area, thus enhancing the interaction between particles and the gas flow within the VRM working chamber. The system was modified using two different configurations. The first configuration involves the installation of a single air splitter at the inlet channel to direct the gas flow more precisely into the grinding chamber. The second configuration builds upon the first by incorporating an air deflector at the rear section of the chamber, combined with the air splitter. This modification is intended to control the overall gas distribution and improve the efficiency of particle transport to the outlet channel. Implementing

these modifications aims to improve the grinding process efficiency and the particle size distribution within the system. A comparison between the standard VRM configuration (a), the air splitter modification (b), and the combination of air splitter and air deflector (c) is presented in Figure 3.

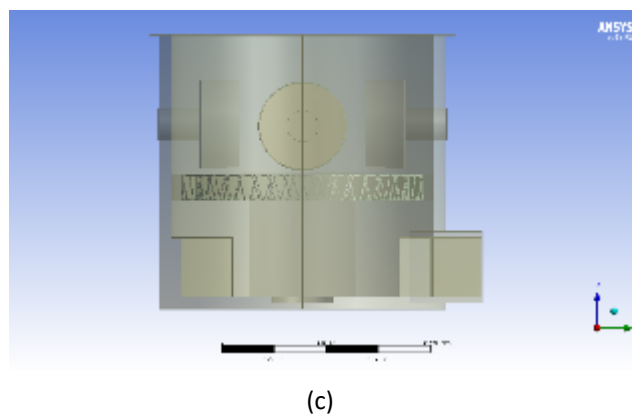
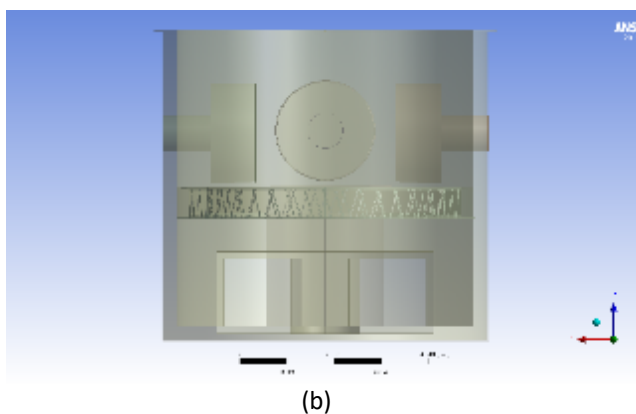
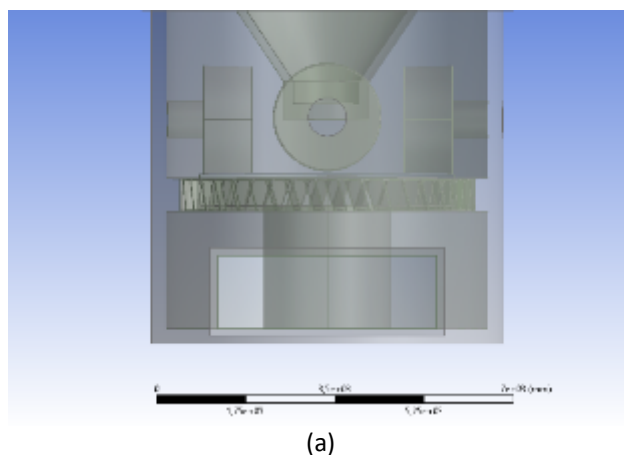


**Fig. 3.** Geometry (a) VRM before modification, (b) VRM with the addition of an air splitter, (c) VRM with the addition of both an air splitter and an air deflector.

## 2.2 Mesh

The meshing process was done using Computational Fluid Dynamics (CFD) based simulation software, ANSYS 2019 R3. In this stage, the flow domain was divided into several discrete three-dimensional elements, forming a mesh structure that represents the control volume of the flow. The mesh generation is a critical step in developing the numerical model for simulation, as it ensures the accuracy of calculations related to particle distribution and interactions within the system.

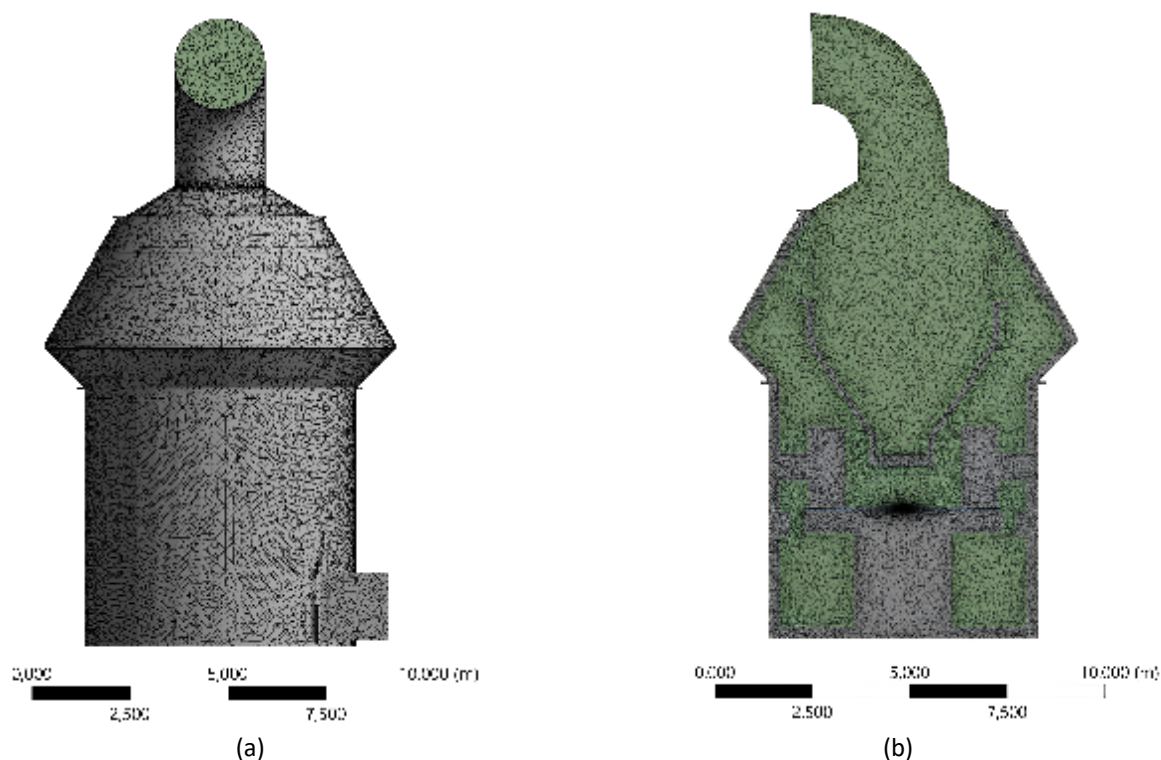


**Fig. 4.** VRM mesh model (a) exterior (b) interior

The mesh used in the simulation consists of tetrahedral elements with an average size of 0.1 meters. This size was chosen to balance the accuracy of the simulation results and computational efficiency. The mesh is locally refined using techniques to capture flow details in areas with high velocity and pressure gradients, such as around the grinding table, nozzle ring, and gas inlet. The mesh generation process resulted in 560,453 nodes and 2,740,261 elements in the simulation domain. A mesh independence study was conducted to ensure that the simulation results are not significantly dependent on mesh density. This study involved comparing several variations in element size until conditions were obtained where changes in mesh size no longer significantly impacted key output parameters, such as pressure distribution, flow velocity, and particle movement patterns.

### 2.3 Boundary Condition

Based on actual operational data from the Vertical Roller Mill (VRM) unit, the gas flow velocity at the inlet is set at 15 m/s. The grinding table rotates at a constant speed of 26 rpm, generating centrifugal force that pushes the ground particles toward the table's edge. After being pushed toward the edge of the grinding table due to centrifugal force, the ground particles are carried along with the gas flow toward the system's outlet. During their movement, the interaction between the particles and the wall surface is considered a perfectly elastic collision, with the wall using a standard wall function and no-slip conditions. Detailed information regarding the boundary conditions applied can be found in Table 2.

**Table 2**  
Boundary conditions of the VRMs

Parameter	Gas	Solid	Value
Inlet of Air	Pressure-inlet	Escape	15 m/s
Inlet of Particles	Wall	Trap	0.1 m/s
Outlet	Pressure-outlet	Escape	0 Pa

The inlet pressure conditions for the gas phase were determined using the turbulence intensity and hydraulic diameter specification method with a turbulence intensity value of 5% and a hydraulic diameter of 1 meter. This approach was chosen to produce representative turbulent flow conditions at the inlet because this area's flow characteristics significantly influence the velocity distribution and direction of particle movement within the grinding chamber. Using these parameters also supports the stability and accuracy of simulations in fluid dynamics modelling in critical areas of the system.

#### 2.4 Solver Setting

The flow simulation was performed using the  $k$ – $\omega$  Shear Stress Transport (SST) turbulence model, which effectively predicts flow characteristics near solid surfaces, especially in conditions with high-velocity gradients such as in grinding table areas. This model combines the advantages of the  $k$ – $\epsilon$  approach for free-zone flow with the accuracy of the  $k$ – $\omega$  model in handling phenomena near walls. This combination makes the SST  $k$ – $\omega$  model highly suitable for systems with complex geometries and significant boundary layer development, such as VRM grinding configurations. The turbulent kinetic Eq. (1) obtained for the simulation are as follows [13]:

$$\frac{\partial \rho k}{\partial t} + \frac{\partial}{\partial x_j} \left[ \rho u_j k - (\mu_L + \sigma_k \mu_T) \frac{\partial k}{\partial x_j} \right] = \tau_{ij} S_{ij} - \beta^* \rho k \omega \quad (1)$$

with the specific dissipation rate Eq. (2) ( $k\omega$  SST):

$$\frac{\partial \rho \omega}{\partial t} + \frac{\partial}{\partial x_j} \left[ \rho u_j \omega - (\mu_L + \sigma_\omega \mu_T) \frac{\partial \omega}{\partial x_j} \right] = P_\omega - \beta \rho \omega^2 + 2(1 - F_1) \frac{\rho \sigma_\omega^2}{\omega} \frac{\partial k}{\partial x_j} \frac{\partial \omega}{\partial x_j} \quad (2)$$

Solid phase modelling in this simulation was performed using the Discrete Phase Model (DPM) with a one-way coupling approach, based on the consideration that the volume fraction of particles relative to the fluid was at a low level so that the effect of particles on the main flow field could be ignored.

**Table 3**  
Point properties of the particles

Point properties	
Variable diameter (m)	0.07
Velocity Magnitude (m/s)	0.1
Total Flow (kg/s)	1e-20

According to actual data from the grinding unit at cement industry facilities in Indonesia, parts are assumed to have a uniform size with a diameter of 7 cm. The particles' physical characteristics follow cement clinker's properties, including density values and restitution coefficients used to model elastic interactions between particles and wall surfaces.

Sampling particles from the VRM during the production process not only ensures a more accurate particle distribution in numerical simulations but also improves the accuracy of simulation results. The expression for the Rosin-Rammler distribution is shown in Eq. (3) [14]:

$$Y_d = \left[ e^{-\left(\frac{d}{d_m}\right)^n} \right] \quad (3)$$

Based on Newton's second law, the motion of a particle is described by the Eq. (4) and Eq. (5):

$$m_p \frac{d\vec{v}_p}{dt} = \vec{F}_l \quad (4)$$

$$\frac{d\vec{x}_l}{dt} = \vec{V}_p \quad (5)$$

Where,  $\vec{F}_l$  is the force acting on a particle. In this simulation, only gravitational force and drag force are considered, and the drag formula is as follows:

$$\vec{F}_D = \frac{18\mu C_D \text{Re}_p}{\rho_p d_p^2} (\vec{u}_l - \vec{v}_p) \quad (6)$$

$$\text{Re}_p = \frac{\rho d_p |\vec{u}_l - \vec{v}_p|}{\mu} \quad (7)$$

$$C_D = \frac{\text{Re}_p}{24} < 1 \quad (8)$$

$$C_D = \frac{\text{Re}_p}{24} \left( 1 + \frac{1}{6} \text{Re}_p^{2/3} \right) 1 \leq \text{Re}_p < 1000 \quad (9)$$

$$C_D = 0.424 \text{Re}_p \text{Re}_p \geq 1000 \quad (10)$$

A Coupled Solver scheme is used to solve the momentum and pressure equations simultaneously, improving numerical stability and accelerating the convergence process, especially in complex flow simulations. The flow field initialization process uses the Least Squares Cell-Based Initialization method to generate more precise initial velocity and pressure distributions based on the existing mesh structure. Additionally, Hybrid Initialization is applied to ensure the initial stability of the numerical solution. As an initial step, the iteration process is run for 1,000 steps to ensure the stability of the flow solution before the particle phase is introduced into the simulation domain.

The success of the Discrete Phase Model (DPM) simulation in ANSYS Fluent depends heavily on the model's ability to realistically describe particle behavior and predict particle capture rates with high precision. One of the main parameters used to evaluate this performance is collection efficiency ( $\eta$ ), which describes the ratio of the mass (or number) of particles successfully captured to the total number of particles injected into the simulation domain. For mass-based approaches, this collection efficiency can be mathematically expressed as [15]:

$$\eta = \frac{N_{\text{catch}}}{N_{\text{injected}}} \times 100\% \quad (11)$$



### 3. Results

#### 3.1 The Effect of Modifying Vertical Roller Mills with Air Splitters and Air Deflectors on Air Velocity Distribution

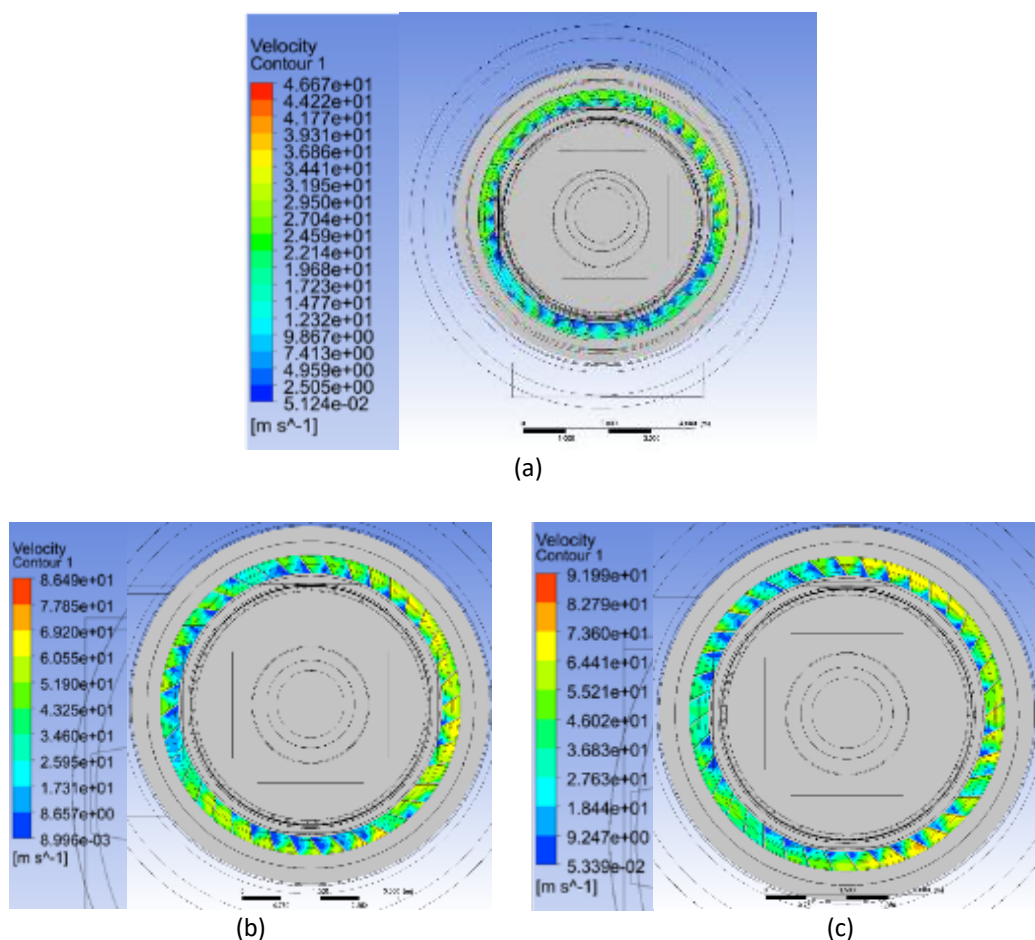


**Fig. 5.** Contour velocity profile (a) before modification, (b) modification with air splitter, (c) modification with air splitter and air deflector

The simulation results in Figure 5 show that modifications with an air splitter and a combination with an air deflector can increase the flow velocity around the nozzle ring outlet. This increase in velocity can be explained by the fact that both modifications help to focus the airflow, reduce turbulence, and direct the flow more controlled, allowing the air to flow more efficiently to the desired area [16]. It is observed that the highest velocity is achieved by the combination modification, as shown in Figure 5(c), where the velocity reaches nearly 90 m/s around the nozzle edge near the inlet and far from the inlet. This demonstrates the effectiveness of adding an air splitter and an air deflector in improving airflow performance. The velocity distribution between the two modifications, adding an air splitter Figure 5(b) and combining an air splitter with an air deflector Figure 5(c) is quite good compared to the normal condition (before modification), which shows a more scattered and uneven velocity distribution. Under normal conditions, it is observed that the air velocity tends to be poorly focused, resulting in suboptimal velocity distribution with greater variations in velocity along the nozzle surface. This could cause flow imbalance, reduce efficiency and increasing the likelihood of turbulence or performance degradation [17]. One of the key benefits of adding this component is its ability to prevent particles in the hot airflow from falling back onto the grinding table due to

uneven velocity [18]. In this case, the modified combination of the air splitter and air deflector outperforms the standard version, which exhibits less optimal velocity distribution.

### 3.2 The Effect of Modifying Vertical Roller Mills with Air Splitters and Air Deflectors on Turbulent Viscosity

Turbulent viscosity models the effects of mixing and energy dissipation due to turbulence in fluid flow. An increase in turbulent viscosity can accelerate particle transport, causing more particles to be pushed out [19].

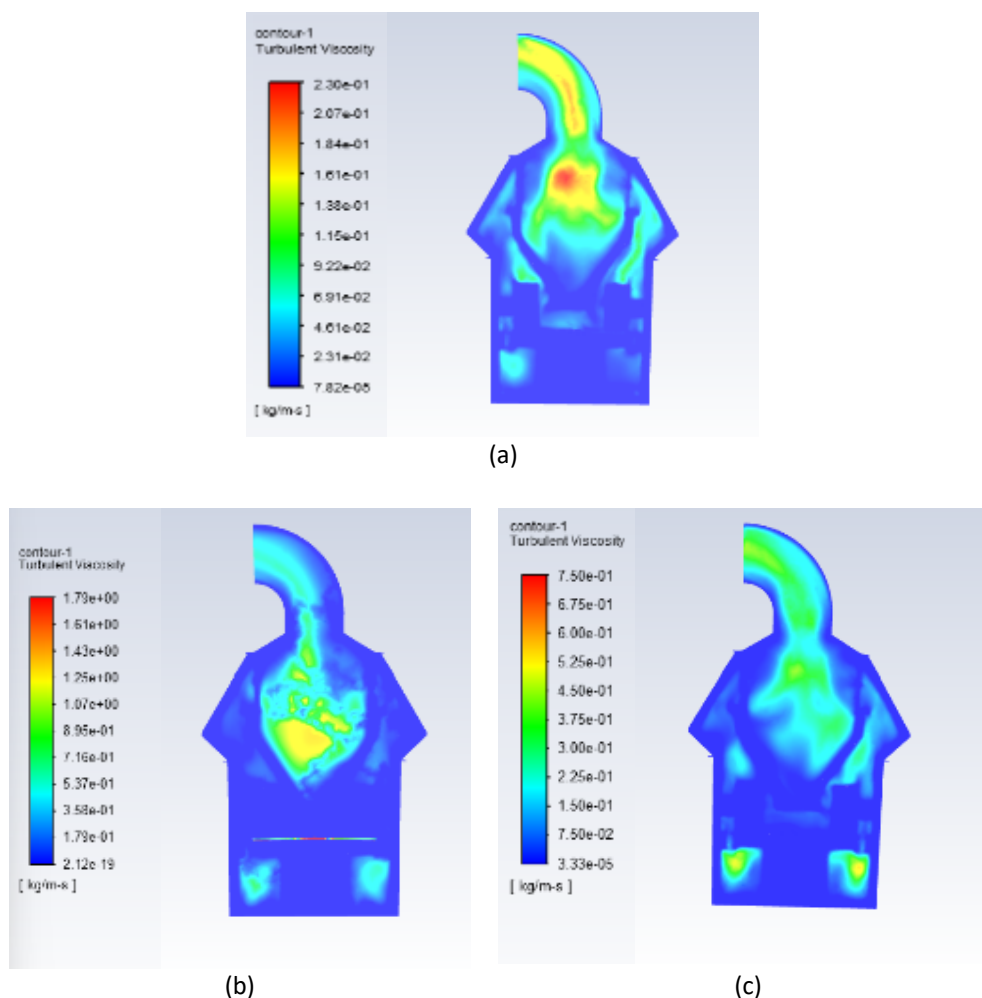


**Fig. 6.** Contour velocity profile (a) before modification, (b) modification with air splitter, (c) modification with air splitter and air deflector

The simulation results in Figure 6 show that the modification with the addition of an air splitter Figure 6(b) produces the highest turbulent viscosity, namely  $7.50\text{e-}01 \text{ kg/m}\cdot\text{s}$ , compared to the normal condition Figure 6(a), which only has a value of around  $2.12\text{e-}19 \text{ kg/m}\cdot\text{s}$ . This increased viscosity indicates that the airflow becomes more turbulent, enhancing energy mixing and accelerating particle transport out of the system [19]. Although the air splitter modification has the highest turbulent viscosity value, its distribution is more uniform in the combined air splitter and air deflector modification Figure 6(c). Nevertheless, the air splitter modification remains more effective in terms of increasing turbulence, which in turn improves airflow performance and minimizes particle

buildup within the system. This results in better mixing, reduces the risk of particle buildup, and enhances transport efficiency and process control [20].

### 3.3 The Effect of Modification Configuration on Particle Efficiency (DPM)

**Table 4**

Particle efficiency calculation

VRM Model	Escape	Total	$\eta_n$ , %
Before modification	7749	22118	35
Modification with Air Splitter	13678	22118	61.84
Modification with an air splitter and an air deflector	9909	22056	45

Modifying the VRM by adding an air splitter and air deflector successfully improved particle efficiency in the raw mill. This is evident from the data in Table 4, where the particle efficiency of the modified air splitter reached 61.84%, a significant increase compared to the pre-modification condition of only 35%. This increase in efficiency represents a difference of 26.84%. Simulation results show that the air splitter modification yields the best results in particle efficiency compared to the combined air splitter and air deflector modification, which has an efficiency of 45%. Higher air velocity can enhance particle lifting efficiency by generating strong turbulence and greater lifting force, making particles easier to detach and transport from the surface [21]. Uneven velocity distribution can cause certain areas to be less effective in capturing or transporting particles [22]. Higher viscosity keeps particles in suspension longer and reduces the settling rate, thereby increasing particle transport efficiency [23]. This makes the modified air splitter more effective due to higher turbulent viscosity and a more focused airflow distribution, enabling more particles to be lifted and transported out of the system more efficiently.

## 4. Conclusions

Based on the simulation results of the third configuration without modification, adding air splitter only, and adding air splitter and air deflector, it can be seen that the addition of a single air splitter provides the best performance in the Vertical Roller Mill; this modification not only focuses the airflow so that the speed approaches 80–85 m/s around the nozzle with a more stable distribution compared to the initial condition, but also produces the highest peak turbulent viscosity value ( $\approx 7.50 \times 10^{-1} \text{ kg/m s}$ ), which indicates optimal mixing of fluid energy and particles, and increases the particle conveying efficiency (DPM) from 35% to around 61.8%, far exceeding the combination of splitter + deflector which only reaches around 44.9%, so that the modification by adding only air splitter overall provides the most significant improvement in particle transport, flow stability, and turbulence distribution in the grinding chamber.

## Acknowledgement

No grant funded this research.

## References

- [1] Hong, Xingyun, Zhengguo Xu, and Zhenwei Zhang. "Abnormal condition monitoring and diagnosis for coal mills based on support vector regression." *IEEE Access* 7 (2019): 170488-170499. <https://doi.org/10.1109/ACCESS.2019.2955249>

- [2] Hu, Yong, Boyu Ping, Deliang Zeng, Yuguang Niu, Yaokui Gao, and Dongming Zhang. "Research on fault diagnosis of coal mill system based on the simulated typical fault samples." *Measurement* 161 (2020): 107864. <https://doi.org/10.1016/j.measurement.2020.107864>
- [3] Li, Xinwen, Yingchun Wu, Huafeng Chen, Xijiong Chen, Yonggang Zhou, Xuecheng Wu, Linghong Chen, and Kefa Cen. "Coal mill model considering heat transfer effect on mass equations with moisture estimation." *Journal of Process Control* 104 (2021): 178-188. <https://doi.org/10.1016/j.jprocont.2021.06.008>
- [4] Agrawal, V., B. K. Panigrahi, and P. M. V. Subbarao. "Review of control and fault diagnosis methods applied to coal mills." *Journal of Process Control* 32 (2015): 138-153. <https://doi.org/10.1016/j.jprocont.2015.04.006>
- [5] Hu, Hailiang, Yiming Li, Yunlong Lu, Xuejun Wang, and Guiqiu Song. "Study of influencing factors of performance in novel vertical roller mills." *Advances in Engineering Software* 202 (2025): 103858. <https://doi.org/10.1016/j.advengsoft.2024.103858>.
- [6] Ali, Muzammil, Alejandro López, Mehrdad Pasha, and Mojtaba Ghadiri. "Optimisation of the performance of a new vertical roller mill by computational fluid dynamics simulations." *Powder Technology* 433 (2024): 119282. <https://doi.org/10.1016/j.powtec.2023.119282>
- [7] Xu, Zhihao, Zihang Fei, Yusen Zhu, Cheng Wang, Xiuqing Yang, Lei Guo, Gang Xue, and Yanjun Liu. "The Numerical Investigation of Solid-Liquid Two-Phase Flow Characteristics Inside and Outside a Newly Designed 3D Sediment Trap." *Journal of Marine Science and Engineering* 12, no. 1 (2023): 16. <https://doi.org/10.3390/jmse12010016>
- [8] Hu, Hailiang, Yiming Li, Yunlong Lu, Yunlong Li, Guiqiu Song, and Xuejun Wang. "Numerical Study of Flow Field and Particle Motion Characteristics on Raw Coal Vertical Roller Mill Circuits." *Minerals Engineering* 218 (2024): 108997. <https://doi.org/10.1016/j.mineng.2024.108997>
- [9] Liu, Chang, Zuobing Chen, Weili Zhang, Chenggang Yang, Ya Mao, Yongjie Yu, and Qiang Xie. "Effects of blade parameters on the flow field and vertical roller mill classification performance via numerical investigations." *Mathematical Problems in Engineering* 2020, no. 1 (2020): 3290694. <https://doi.org/10.1155/2020/3290694>
- [10] Altun, Deniz, Hakan Benzer, Namik Aydogan, and Carsten Gerold. "Operational parameters affecting the vertical roller mill performance." *Minerals Engineering* 103 (2017): 67-71. <https://doi.org/10.1016/j.mineng.2016.08.015>
- [11] Fatahi, Rasoul, Hadi Abdollahi, Mohammad Noaparast, and Mehdi Hadizadeh. "Investigating the impact of key variables on differential pressure in cement vertical roller Mills, using the GBM algorithm." *Powder Technology* (2025): 121168. <https://doi.org/10.1016/j.powtec.2025.121168>
- [12] Liu, Hao-Ran, Chong Shen Ng, Kai Leong Chong, Detlef Lohse, and Roberto Verzicco. "An efficient phase-field method for turbulent multiphase flows." *Journal of Computational Physics* 446 (2021): 110659. <https://doi.org/10.1016/j.jcp.2021.110659>
- [13] Zhao, Ming, Tong Wei, Shixi Hao, Qiushi Ding, Wei Liu, Xiaojian Li, and Zhengxian Liu. "Turbulence simulations with an improved interior penalty discontinuous Galerkin method and SST k- $\omega$  model." *Computers & Fluids* 263 (2023): 105967. <https://doi.org/10.1016/j.compfluid.2023.105967>
- [14] Hu, Hailiang, Yiming Li, Yunlong Lu, Xuejun Wang, and Guiqiu Song. "Study of influencing factors of performance in novel vertical roller mills." *Advances in Engineering Software* 202 (2025): 103858. <https://doi.org/10.1016/j.advengsoft.2024.103858>
- [15] Papkov, Vyacheslav, Nikita Shadymov, and Dmitry Pashchenko. "CFD-modeling of fluid flow in Ansys Fluent using Python-based code for automation of repeating calculations." *International Journal of Modern Physics C* 34, no. 09 (2023): 2350114. <https://doi.org/10.1142/S0129183123501140>
- [16] Sohn, Jonas, Martynas Liulys, Dafni Despoina Avgoustaki, and George Xydis. "CFD analysis of airflow uniformity in a shipping container vertical farm." *Computers and Electronics in Agriculture* 215 (2023): 108363. <https://doi.org/10.1016/j.compag.2023.108363>
- [17] Vinod, Ashwin, Cong Han, and Arindam Banerjee. "Tidal turbine performance and near-wake characteristics in a sheared turbulent inflow." *Renewable Energy* 175 (2021): 840-852. <https://doi.org/10.1016/j.renene.2021.05.026>
- [18] Hu, Hailiang, Yiming Li, Yunlong Lu, Yunlong Li, Guiqiu Song, and Xuejun Wang. "Numerical Study of Flow Field and Particle Motion Characteristics on Raw Coal Vertical Roller Mill Circuits." *Minerals Engineering* 218 (2024): 108997. <https://doi.org/10.1016/j.mineng.2024.108997>
- [19] Saieed, Ahmed, and Jean-Pierre Hickey. "Viscosity-modulated clustering of heated bidispersed particles in a turbulent gas." *Journal of Fluid Mechanics* 979 (2024): A46. <https://doi.org/10.1017/jfm.2023.1049>
- [20] Brunner, Daniel, Joe Goodbread, Klaus Häusler, Sunil Kumar, Gernot Boiger, and Hassan A. Khawaja. "Analysis of a tubular torsionally resonating viscosity-density sensor." *Sensors* 20, no. 11 (2020): 3036. <https://doi.org/10.3390/s20113036>
- [21] Pandya, Soham, Ramadan Ahmed, and Subhash Shah. "Wellbore cleanout in inclined and horizontal wellbores: the effects of flow rate, fluid rheology, and solids density." *SPE Drilling & Completion* 35, no. 01 (2020): 048-068. <https://doi.org/10.2118/194240-PA>

- [22] Lu, Changxin, Ben Sun, Chengzhi Lang, Jiawei Li, Chengyun Xin, Tuo Zhou, and Tairan Fu. "Numerical investigation on ash deposition and wear performance of integrally-molded double-sided spiral finned tubes for waste heat recovery." *Applied Thermal Engineering* 266 (2025): 125593.  
<https://doi.org/10.1016/j.applthermaleng.2025.125593>
- [23] Chen, Xiaodong, Lele Yang, Lian Luo, Liang Yu, and Zhiyuan Luo. "Effects of fluid properties on coarse particles transport in a vertical pipe." *Powder Technology* 449 (2025): 120421.  
<https://doi.org/10.1016/j.powtec.2024.120421>